Attitude Determination Covariance Analysis for Geostationary Transfer Orbits

Jozef C. Van der Ha*
European Space Operations Centre ESA, Darmstadt, FRG

Fundamental biases in V-slit sun and pencil-beam infrared Earth sensor measurements are identified and modeled in terms of representative covariances. Their effects on attitude determination accuracy are assessed by means of covariance transformations following the calculations involved in a realistic attitude estimation process. The results are useful in identifying the best attitude determination intervals and for providing quantitative estimates of the expected error for selected launch configurations. On this basis the most favorable sensor settings can be selected for a given launch window. This is of particular interest for present-day communication satellites equipped with variable sensor mountings which can be adjusted before launch.

Introduction

TO date, all nine European Space Agency (ESA) satellites successfully launched into geostationary transfer orbit were spin stabilized. The accuracy with which the spin axis orientation can be determined is of crucial importance. Attitude determination errors, namely, result in orbit injection errors during apogee motor firing (AMF) which need to be corrected by means of the normal-mode reaction control system afterward. There is a strong incentive to minimize the fuel required for these so-called acquisition maneuvers since any savings achieved here result directly in a prolongation of the prospective mission lifetime.

The spin axis attitude determination of these satellites is based on measurements resulting from V-slit sun sensors and pencil-beam infrared Earth sensors. It is evident that the accuracy of the attitude estimate depends critically on the inherent modeling errors of the sensor signals. Two classes of measurement errors may be distinguished, i.e., random and systematic errors. The former class of errors is the result of stochastic fluctuations in the realization of a particular measurement induced, for instance, by limitations in the precision of the sensing instrumentation. To a lesser extent, the quantization in the onboard registration of the measurement data also plays a role. It is essential to recognize that the influence of random errors on the estimation accuracy can essentially be eliminated by simply considering a sufficiently large batch of measurement data.

On the other hand, systematic errors are far more serious since their adverse influence on the estimation accuracy cannot be removed in a straightforward manner. The sources for this type of error are manyfold: sensor mounting misalignments, electronic triggering delays, spin axis tilt with respect to the designed spin axis, sensor calibration offsets, infrared profile modeling errors due to seasonal or local variations, and orbit determination, or sun ephemeris errors. In principle, an extended state model could be devised containing certain well-selected biases to be estimated along with the attitude angles. It should be recognized, however, that the observability of individual state parameters to be estimated becomes problematic if all relevant biases are included in the state model. For isolated biases this approach has been followed in a few cases (e.g., see Ref. 1, Secs. 13.2 and 14.2), but, in general, the implementation of a quick and reliable bias estimation in operational software is extremely difficult.

In any case, it is of interest to understand the characteristics of the propagation of measurement biases into the resulting attitude estimate. This knowledge would allow the selection of favorable sensor settings and attitude determination intervals in order to minimize the adverse effects induced by systematic measurement errors. In the present paper, a method is presented which allows the calculation of the covariances of the attitude angles on the basis of representative variances of all relevant measurement biases. The results are useful for analyzing the sensitivity of error magnification to sensor design parameters (e.g., alignments) and geometrical configurations (e.g., sun-Earth colinearity). Provided that the choice of input bias covariances is realistic, a quantitative assessment of the attitude error to be expected in a particular configuration is established. It should be recognized that the effect of a particular bias on the attitude determination result typically would vary only slowly in relation to the measurement sample period. Therefore, the error covariances obtained from a single-frame attitude determination method[1,2] can often be considered representative of the error from a small batch of measurement data as well.

The study is of particular importance for selecting optimal sensor settings for ESA's European Communications Satellite (ECS)-type communication satellites equipped with variable sensor mountings which can be adjusted (within a range of 19 deg) before launch. The benefits are not insignificant: improvement in attitude knowledge at apogee motor firing by as little as 0.13 deg may well translate into a lifetime extension on the order of one month.

Modeling of Sensor Measurement Biases

Sensor measurements consist of the registration of event times corresponding to the sun sensor meridian and skew slits crossing the center of the sun's disk and the Earth sensor pencil-beams crossing the Earth's horizon. Since measurements normally can be processed onboard from at most two pencil-beams simultaneously, there are typically four or six discrete event times available over one spin period: t_0, t_1: sun sensor meridian, skew slit event times; t_2, t_3: first pencil-beam horizon in, out events; and t_4, t_5: second pencil-beam horizon in, out events.

In a typical sequence of events in transfer orbit three different coverage intervals may be distinguished: 1) the first pencil-beam has coverage, 2) both beams have coverage, 3)

Presented as Paper 84-1882 at the AIAA Guidance and Control Conference, Seattle, WA, Aug. 20-22, 1984; submitted Oct. 8, 1984; revision received July 26, 1985. Copyright © American Institute of Aeronautics and Astronautics, Inc., 1984. All rights reserved.

*Senior Analyst, Orbit Attitude Division. Member AIAA.

only the second beam has coverage. The sun sensor, of course, normally has coverage over the whole transfer orbit.

In the on-ground processing of the event times the sun meridian slit crossing time t_0 is taken as reference in the calculation of the rotation angles:

$$y_j = \omega(t_j - t_0), \qquad j = 1,\ldots,5 \tag{1}$$

where ω is the constant spin rate. The rotation angles $y = (y_1,\ldots,y_5)^T$ are directly related to the angular measurements φ, α, and κ shown in Figs. 1 and 2:

$$y = (\varphi,\ \alpha_1 - \kappa_1, \alpha_1 + \kappa_1, \alpha_2 - \kappa_2, \alpha_2 + \kappa_2)^T \tag{2}$$

The angle φ designates the rotation angle between the sun occurrence in the meridian and skew slits, α_i refers to the sun/Earth azimuth angle as measured by the ith pencil-beam, and κ_i is the corresponding Earth's half-chordlength angle.

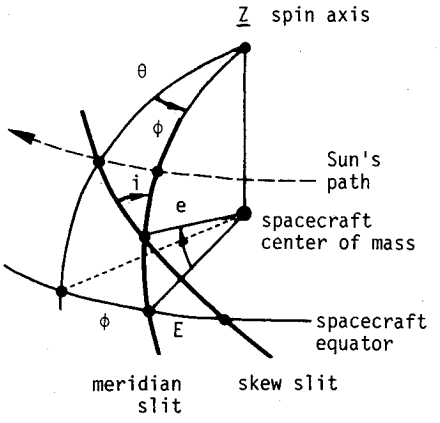

Fig. 1 Geometry of sun sensor measurement φ.

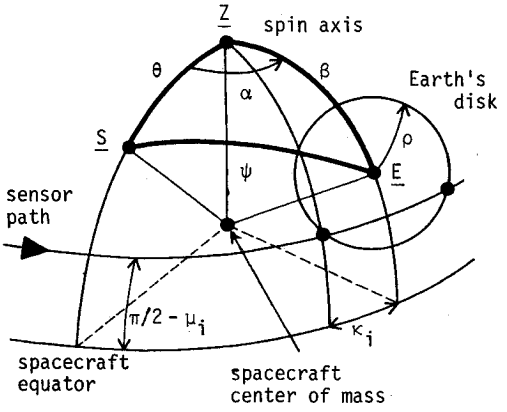

Fig. 2 Geometry of Earth sensor measurements α_i and κ_i.

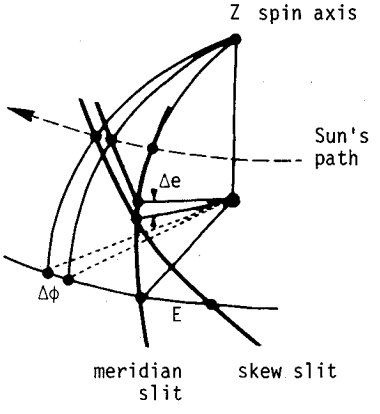

Fig. 3 Effect of slit intersection bias Δe on measurement φ.

Sun Sensor Measurement Biases

Sun sensor measurement biases may be categorized according to the following error sources:

1) Optical bias designates the offset in the electronically registered sun crossing event time relative to the ideal event time, i.e., when the center of the sun's disk crosses the centerline of the sun sensor slits. The differential bias between meridian and skew pulse registration [estimated at 0.1 deg (3σ)] directly affects the φ rotation angle measurement, whereas a uniform delay (of similar order) leads to a sun/Earth azimuth bias.

2) Mounting error is due to alignment imperfections. A mounting offset in a direction along the meridian slit plane would directly result in a measurement bias in the φ rotation angle, Fig. 3. On the other hand, a mounting displacement along the spacecraft equator plane would introduce a sun/Earth azimuth angle bias (unless the pencil-beams are subjected to the same misalignment).

3) Elevation error refers to a rotation of the sensor planes such that the spin axis does not lie in the meridian slit plane. This type of bias is less serious than the previous one provided that the sun crosses near the intersection of the slits.

4) Spin axis tilt describes the offset of the actual dynamic spin axis relative to the designed geometrical Z axis. Although spacecraft balancing specifications usually require a tilt angle of less than 0.1 deg, microgravity conditions may lead to a larger in-flight value. The spin axis tilt deviation can be broken up into components along and normal to the meridian slit. The former component is effectively identical to the first type of mounting error in type 2, whereas the latter amounts to an elevation error as described in type 3. For both components 0.12 deg (3σ) is taken, which includes the relatively less significant pure mounting errors.

5) Differential slit separation error is caused by slit manufacturing irregularities and is taken as 0.02 deg (3σ).

Other error sources (e.g., ephemeris errors) are ignored here because they are clearly less significant. Also nutation effects are excluded as these have a random noise character with mean value zero (except in case of commensurability between spin and nutation frequencies).

The results are now summarized by the following offsets:

$$\Delta e = 0.12 \text{ deg},\ \Delta\epsilon = 0.12 \text{ deg},\ \Delta i = 0.02 \text{ deg},\ \Delta\tau = 0.1 \text{ deg } (3\sigma) \tag{3}$$

Here, Δe is the slit intersection offset within the meridian slit plane (types 2 and 4), as shown in Fig. 3; $\Delta\epsilon$ the elevation error (types 3 and 4) and is shown in Fig. 4; Δi the differential slit misalignment ν visualized in Fig. 5; $\Delta\tau$ denotes the differential angular bias between the meridian and skew event pulses (type 1) so that $\Delta\tau = \Delta\varphi_1$. The uniform delays or mounting offsets of types 1 and 2 will be incorporated in the Earth sensor error budget.

The subsequent mathematical analysis will use the fact that the four systematic biases listed in Eqs. (3) can be considered to be statistically uncorrelated.

Earth Sensor Measurement Biases

Earth sensor measurement biases may be classified as follows:

1) Spin axis tilt is naturally correlated to the same effect encountered previously and is described by the same parameters, Δe and $\Delta\epsilon$, as given in Eqs. (3); however, the contribution of pure sun sensor mounting errors has been included in these values. Since Earth and sun sensors are usually contained in the same physical box their differential mounting error may be

considered negligible in comparison to the total (combined) mounting offsets and spin axis tilt effects. It can be shown that the effect of the $\Delta\epsilon$ tilt component is negligible in first order so that only Δe has an effective contribution to the Earth sensor measurements.

2) Sensor pointing error contains actual pencil-beam mounting and optical axis offsets and may be decomposed in a component $\Delta\mu$ of order 0.05 deg (3σ) in sensor inclination (Fig. 1) and another one of the same order along the scanning direction resulting in a sun/Earth azimuth bias.

3) Delay bias represents imperfections in predicted (after calibration) and realized event pulses. Also Earth oblateness effects and infrared profile asymmetries may contribute to this bias. It will be modeled as a uniform delay (again leading to a sun/Earth azimuth error) and a differential delay of magnitude $\Delta b = 0.2$ deg (3σ). The total sun/Earth azimuth bias accumulated from delay and pointing errors as well as sun sensor meridian slit offsets is estimated to be $\Delta d = 0.25$ deg (3σ). Due to the so-called Pagoda effect (e.g., Ref. 1), the differential delay errors increase sharply near the edges of the coverage interval.

4) Apparent Earth radius offset describes the radially symmetric infrared profile error. On the basis of 15 km (3σ) uncertainty in the Earth infrared horizon at which triggering occurs, one may express $\Delta\rho$ as a linear function of true anaomaly ν over the coverage interval:

$$\Delta\rho = 0.02 + 5\times 10^{-4}\,|180-\nu|\,\text{deg} \tag{4}$$

The orbit determination error contribution to $\Delta\rho$ can be shown to be relatively insignificant.

5) Sun/Earth angle bias originates from sun ephemeris errors (e.g., parallactic effects due to satellite/Earth relative motion) and orbit determination error components. As the angular position uncertainty is less than 0.03 deg in the apogee region and the sun ephemeris error is about 0.02 deg, a total value of $\Delta\psi = 0.05$ deg (3σ) appears conservative.

In summary, the following additional biases have been introduced:

$$\Delta d = 0.25 \text{ deg}, \quad \Delta\mu = 0.05 \text{ deg}, \quad \Delta b = 0.2 \text{ deg}$$

$$\Delta\rho\,[\text{Eq. (4)}], \quad \Delta\psi = 0.05 \text{ deg } (3\sigma) \tag{5}$$

Relationships Between Sensor Measurements and Biases

The rotation angles y_j, $j = 1,\ldots,5$, of Eqs. (1) and (2) represent the fundamental measurements resulting from the sun and Earth sensor event pulses. The linearized functional relationship between the five-dimensional array of measurement errors Δy and the corresponding nine-dimensional array of biases Δb listed successively in Eqs. (3) and (5) is expressed as

$$\Delta y = [M]\Delta b \tag{6}$$

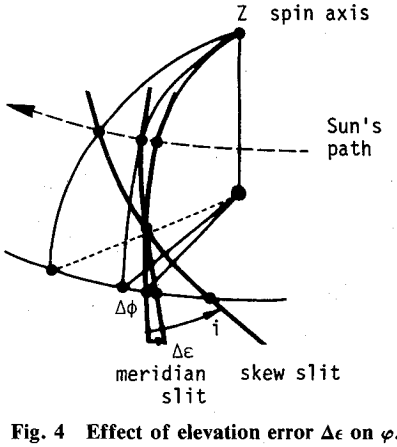

Fig. 4 Effect of elevation error $\Delta\epsilon$ on φ.

The components of the 5×9 matrix $[M]$ can be calculated by means of spherical geometry[3]:

$$[M] = \begin{bmatrix} -f_e & f_1-f_0 & f_1 & 1 & 0 & 0 & 0 & 0 & 0 \\ h_1 & -f_0 & 0 & 0 & 1 & -h_1 & -c_1 & -p_1 & p_\psi \\ -h_1 & -f_0 & 0 & 0 & 1 & h_1 & d_1 & p_1 & p_\psi \\ h_2 & -f_0 & 0 & 0 & 1 & -h_2 & -c_2 & -p_2 & p_\psi \\ -h_2 & -f_0 & 0 & 0 & 1 & h_2 & d_2 & p_2 & p_\psi \end{bmatrix} \tag{7}$$

with functions

$$f_e = \cos e \tan i \cos^2 E + \sin e \tan(\phi+E)\,[1/\cos e + (\cos e)/A^2]$$

$$f_0 = A\sin(\phi+E) - \sin e$$

$$f_1 = \cos i \tan(\phi+E)/(A^2\sin^3 i) - \sin e \cos^2 E/\cos^2 i$$

$$h_i = \{\cos\mu_i \sin\beta \cos\kappa_i - \sin\mu_i \cos\beta\}$$

$$\div(\sin\mu_i \sin\beta \sin\kappa_i), \qquad i = 1,2$$

$$c_i = 1 + c(1-\kappa_i/\kappa_{i,\max}), \qquad i = 1,2$$

$$d_i = 1 + d(1-\kappa_i/\kappa_{i,\max}), \qquad i = 1,2$$

$$p_i = \sin\rho/(\sin\mu_i \sin\kappa_i \sin\beta), \qquad i = 1,2$$

$$p_\psi = \sin\theta \sin\alpha/(\sin\psi \sin\beta) \tag{8}$$

The constants A and E are defined as

$$A = (\sin^2 e + \cot^2 i), \qquad E = \arctan(\sin e \tan i) \tag{9}$$

The constants c and d govern the extent of the Pagoda effect on the differential delay bias as a function of the chordlength and are taken to be equal to 2. Simulations have shown a low sensitivity to the value chosen as long as symmetry is preserved. The asymmetry starts only close to the edge of the Earth's disk where the data should be discarded in any case, cf. Wertz,[1] §9.4. The meaning of the remaining symbols appearing in Eqs. (8) is obvious from Figs. 1-5.

Since the nine biases are uncorrelated the 5×5 covariance matrix of the fundamental measurement y follows from Eq. (6):

$$[\text{cov}(y)] = E\{\Delta y \cdot \Delta y^T\} = [M] \begin{bmatrix} \sigma_e^2 & & 0 \\ & \ddots & \\ 0 & & \sigma_\psi^2 \end{bmatrix} [M]^T$$

or

$$[\text{cov}(y)]_{ij} = \sum_{k=1}^{9} M_{ik} M_{jk} \sigma_k^2 \tag{10}$$

where $\sigma_1 = \sigma_e, \ldots, \sigma_9 = \sigma_\psi$ represents the standard deviations corresponding to the biases as introduced in Eqs. (3) and (5).

Propagation of Measurement Covariances

The error covariance matrix of the fundamental rotation angle measurements y has been established above on the basis of the selected sensor measurement biases. Subsequently, the covariances of the derived observation angles θ, β, and α (i.e., solar aspect angle, Earth colatitude, and sun/Earth azimuth angle, respectively) will be calculated. These angles form the essential inputs in to the attitude estimation model to be considered subsequently.

Table 1 Variation of 3σ declination error over the launch window for three sensor settings

Sensor settings, deg	Launch time (hr:min GMT)				
	12:00	12:30	13:00	13:30	14:00
2.5; −1.5	0.31	0.47	0.62	0.49	0.34
8.5; 4.5	0.23	0.36	0.51	0.62	0.44
13.5; 9.5	0.19	0.26	0.40	0.57	0.56

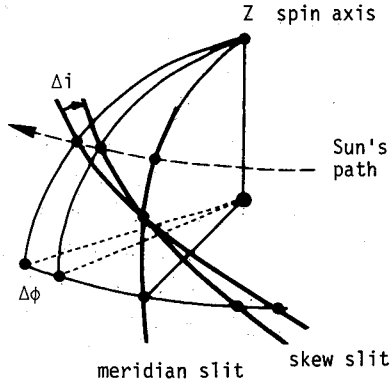

Fig. 5 Effect of differential slit misalignment Δi on φ.

Covariance Matrix of θ, κ, and α

As a first step in the transformation from the rotation angle measurements y in Eq. (2) to the angles θ, β, and α, the array

$$\gamma = (\theta, \kappa_1, \alpha_1, \kappa_2, \alpha_2)^T \tag{11}$$

is introduced. The solar aspect angle θ follows directly from the measurement $y_1 = \varphi$ according to

$$\theta(\phi) = \arctan\{\cos e / [A \sin(\phi + E)]\} \tag{12}$$

The propagation of the measurement error $\Delta y_1 = \Delta\varphi$ into the solar aspect angle is governed by the following linearized relationship:

$$\Delta\theta = \frac{\partial\theta}{\partial\phi}\Delta\phi = g(\phi)\Delta\phi \tag{13}$$

with

$$g(\varphi) = -\sin\theta(\phi)\ \cos\theta(\phi)\ \cot(\phi + E) \tag{14}$$

The function $g(\varphi)$ may be interpreted as the sensitivity coefficient describing the magnification of a measurement error $\Delta\varphi$ into the resulting $\Delta\theta$ and is of the order of 1.8 for a slit separation of 28 deg and a solar aspect angle in the range of 75-105 deg.

The transformation matrix describing the relation $\Delta\gamma = [\partial\gamma/\partial y]\Delta y$ can be shown to be

$$[N] = \left[\frac{\partial\gamma}{\partial y}\right] = 0.5 \begin{bmatrix} 2g & 0 & 0 & 0 & 0 \\ 0 & -1 & 1 & 0 & 0 \\ 0 & 1 & 1 & 0 & 0 \\ 0 & 0 & 0 & -1 & 1 \\ 0 & 0 & 0 & 1 & 1 \end{bmatrix} \tag{15}$$

The covariance matrix of γ can now readily be expressed in that of y:

$$[\mathrm{cov}(\gamma)] = [N]\,[\mathrm{cov}(y)]\,[N]^T \tag{16}$$

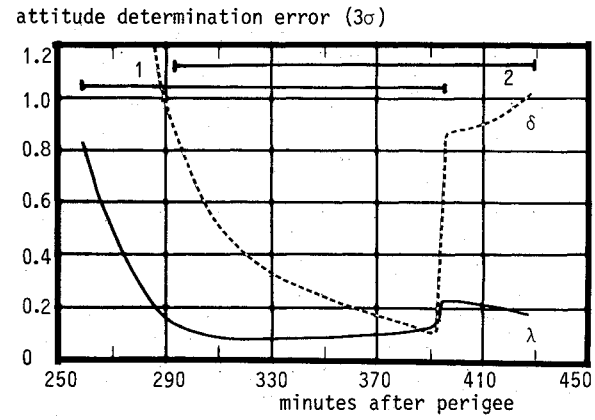

Fig. 6 Expected attitude determination error (3σ) over sensor coverage interval for a launch date of March 21 and reference attitude with right ascension $\lambda = 280$ deg and declination $\delta = -7$ deg. (The curves indicated by λ and δ refer to the evolution of the errors in right ascension and declination, respectively. The bars labeled 1 and 2 designate the extent of the coverage intervals of the pencil-beams 1 and 2, respectively.)

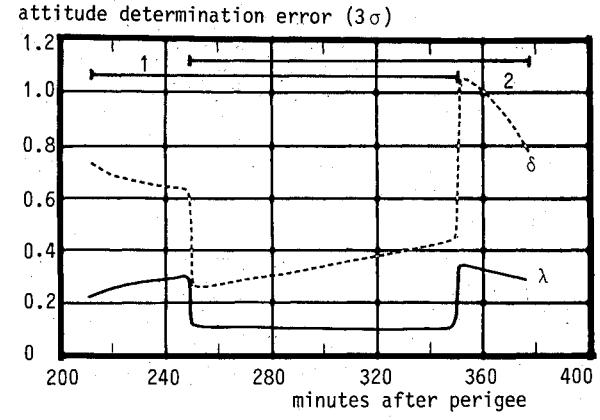

Fig. 7 Expected attitude determination error (3σ) for a launch date of May 15, and reference attitude $\lambda = 307$ deg, $\delta = -7$ deg. Sensor settings are 2.5 and −1.5 deg (refer to Fig. 6 for clarifications).

Covariance Matrix of θ, β, and α

Subsequently, the observation angles θ, β, and α are determined from the array of five derived measurements γ. Here two different situations must be considered, namely, 1) where Earth sensor measurements are available from one pencil beam only, and 2) where both beams have coverage.

Calculation of β and α from Two Beams

In this case all five entries in the array γ of Eq. (11) are available. For the determination of β four equations are at our disposal (cf., Fig. 1):

$$\cos\mu_i\cos\beta + \sin\mu_i\cos\kappa_i\sin\beta = \cos\rho$$

$$\cos\theta\cos\beta + \sin\theta\cos\alpha_i\sin\beta = \cos\psi \qquad i = 1,2 \tag{17}$$

The objective is to determine β in such a manner that its variance is minimal on the basis of the given covariances for the input observation angles θ, κ_i, and α_i. It should be noted that the uncertainties in the angles ρ, ψ, and μ_i appearing in Eqs. (17) have been taken into account when establishing the covariances of θ, κ_i, and α_i from the basic measurement biases. A different approach is taken in Ref. 4, where fundamental biases are assigned to all input variables only at this stage.

The system of equations (17) is written in compact vector notation as

$$\boldsymbol{a}\cos\beta+\boldsymbol{b}\sin\beta-\boldsymbol{c}=\boldsymbol{0} \tag{18}$$

with obvious entries in the four-dimensional arrays $\boldsymbol{a}$, $\boldsymbol{b}$, and $\boldsymbol{c}$. Introducing weighting factors w_j, $j=1,\ldots,4$, for each of the four equations, one obtains the following combined system:

$$A\cos\beta+B\sin\beta-C=0 \tag{19}$$

where $A=\boldsymbol{w}^T\cdot\boldsymbol{a}$, $B=\boldsymbol{w}^T\cdot\boldsymbol{b}$, and $C=\boldsymbol{w}^T\cdot\boldsymbol{c}$. After determination of $\boldsymbol{w}$ the solution of β is given by

$$\beta=\arctan(B/A)\pm\arccos\{C/\sqrt{(A^2+B^2)}\} \tag{20}$$

The sign ambiguity can be resolved by a consistency check with the individual solutions of each of the four equations or by a priori knowledge of the β angle.

The array elements of $\boldsymbol{a}$ and $\boldsymbol{b}$ (and thus the scalars A and B) contain the observation angles $\boldsymbol{\gamma}=(\theta,\ \kappa_1,\ \alpha_1,\ \kappa_2,\ \alpha_2)^T$. In order to establish the transformation from $\Delta\boldsymbol{\gamma}$ to $\Delta\beta$, Eq. (19) is written in shorthand as

$$F(\beta,\boldsymbol{\gamma})=\boldsymbol{w}^T\cdot\boldsymbol{f}(\beta,\boldsymbol{\gamma})=0 \tag{21}$$

with $\boldsymbol{f}$ defined by Eq. (18). By differentiation, one obtains

$$\Delta\beta=-(\nabla F^T\cdot\Delta\boldsymbol{\gamma})\Big/\frac{\partial F}{\partial\beta}\qquad\nabla=\frac{\partial}{\partial\boldsymbol{\gamma}} \tag{22}$$

One can now calculate the variance of β as

$$\sigma_\beta^2=[\nabla F^T\cdot\mathrm{cov}(\boldsymbol{\gamma})\cdot\nabla F]\Big/\left(\frac{\partial F}{\partial\beta}\right)^2 \tag{23}$$

Minimization of σ_β^2 with respect to the four weights w_j can be shown to lead to the linear system[3]

$$[A]\boldsymbol{w}=\boldsymbol{d} \tag{24}$$

with

$$[A]=[P]\cdot[\mathrm{cov}(\boldsymbol{\gamma})]\cdot[P]^T,\qquad[P]=\left[\frac{\partial\boldsymbol{f}}{\partial\boldsymbol{\gamma}}\right] \tag{25}$$

$$\boldsymbol{d}=\frac{\partial\boldsymbol{f}}{\partial\beta}=\boldsymbol{b}\cos\beta-\boldsymbol{a}\sin\beta \tag{26}$$

The 4×5 matrix $[P]$ has the following nonzero entries:

$$\begin{aligned}
&P_{12}=-\sin\mu_1\sin\kappa_1\sin\beta, && P_{24}=-\sin\mu_2\cos\kappa_2\sin\beta\\
&P_{33}=-\sin\theta\ \sin\alpha_1\sin\beta, && P_{45}=-\sin\theta\ \sin\alpha_2\sin\beta\\
&P_{31}=\cos\theta\ \cos\alpha_1\sin\beta-\sin\theta\ \cos\beta\\
&P_{41}=\cos\theta\ \cos\alpha_2\sin\beta-\sin\theta\ \cos\beta
\end{aligned} \tag{27}$$

By the nature of the covariance transformations the 4×4 matrix $[A]$ must be symmetric. Furthermore, $[A]$ is nonsingular, since, on one hand, the two pencil-beam inclinations μ_i $(i=1,2)$ are different, leading to different κ_i observations and corresponding entries in the matrix $[P]$. The observations α_1 and α_2, on the other hand, represent the same physical sun/Earth angle so that the corresponding elements of $[P]$ in Eqs. (27) are almost identical. For these two equations independence follows from the different biases according to the chordlength-dependent factors c_i and d_i in Eqs. (8).

The weighting factors w_j, $j=1,\ldots,4$, must be calculated from Eq. (24) by numerical means. The transformation $\Delta\boldsymbol{\gamma}$ to $\Delta\beta$ with these weights satisfies the minimum-variance property and is provided by Eq. (22):

$$\Delta\beta=-\boldsymbol{p}^T\cdot\Delta\boldsymbol{\gamma},\qquad\boldsymbol{p}^T=\nabla F^T\Big/\frac{\partial F}{\partial\beta} \tag{28}$$

The calculation of the minimum-variance sun/Earth azimuth angle α from the observations α_1 and α_2 appearing in the array $\boldsymbol{\gamma}$ of Eq. (11) is of a similar nature. Writing $\alpha=q\alpha_1+(1-q)\alpha_2$ with weighting factor q it follows that

$$\sigma_\alpha^2=q^2\gamma_{33}+2q(1-q)\gamma_{35}+(1-q)^2\gamma_{55} \tag{29}$$

where γ_{ij} refers to the entries of the covariance matrix $[\mathrm{cov}(\boldsymbol{\gamma})]$ in Eq. (16). The minimum value of σ_α^2 is reached when

$$q=(\gamma_{55}-\gamma_{35})/(\gamma_{33}-2\gamma_{35}+\gamma_{55}) \tag{30}$$

resulting in

$$\sigma_\alpha^2=(\gamma_{33}\gamma_{55}-\gamma_{35}^2)/(\gamma_{33}-2\gamma_{35}+\gamma_{55}) \tag{31}$$

Designating the observation array $(\theta,\beta,\alpha)^T$ as $\boldsymbol{\eta}$, the resulting transformation from $\Delta\boldsymbol{\gamma}$ to $\Delta\boldsymbol{\eta}$ becomes

$$\Delta\boldsymbol{\eta}=\begin{bmatrix}1&0&0&0&0\\-p_1&-p_2&-p_3&-p_4&-p_5\\0&0&q&0&1-q\end{bmatrix}\Delta\boldsymbol{\gamma}=[Q]\Delta\boldsymbol{\gamma} \tag{32}$$

The 3×3 covariance matrix for the derived angles $\boldsymbol{\eta}$ follows in the usual manner:

$$[\mathrm{cov}(\boldsymbol{\eta})]=[Q]\cdot[\mathrm{cov}(\boldsymbol{\gamma})]\cdot[Q]^T \tag{33}$$

Calculation of β and α from One Beam

In the case where only one of the two pencil beams has coverage, an analysis similar to that shown above can be performed to obtain a minimum-variance estimate for β from Eqs. (17). The angle α of course equals α_1 or α_2, as no redundant information is available. The matrix equation in Eq. (24) contains now only two weighting factors, i.e., w_1 and w_3 or w_2 and w_4. Concentrating on the first case, matrix $[A]$ is given by the nonzero components

$$\begin{aligned}
&A_{11}=P_{12}^2\gamma_{22},\quad A_{13}=A_{31}=P_{12}(P_{31}\gamma_{12}+P_{33}\gamma_{23})\\
&A_{33}=P_{31}^2\gamma_{11}+2P_{31}P_{33}\gamma_{13}+P_{33}^2\gamma_{33}
\end{aligned} \tag{34}$$

In this case, the solution for the weights can be calculated analytically as

$$\begin{bmatrix}w_1\\w_3\end{bmatrix}=\frac{1}{A_{11}A_{33}-A_{13}^2}\begin{bmatrix}A_{33}d_1-A_{13}d_3\\A_{11}d_3-A_{13}d_1\end{bmatrix} \tag{35}$$

The transformation from $\Delta\boldsymbol{\gamma}$ to $\Delta\boldsymbol{\eta}$ is as in Eq. (32) with $p_4=p_5=0$, and $q=1$ in the present case, and $p_2=p_3=0$ and $q=0$ in the case where the other pencil-beam has coverage. The final covariance matrix of $\boldsymbol{\eta}=(\theta,\beta,\alpha)^T$ follows then as in Eq. (33).

Attitude Determination Error Covariances

The observation angles $\boldsymbol{\eta}=(\theta,\beta,\alpha)^T$ represent the essential inputs into the attitude estimation process. The covariance matrix $[\mathrm{cov}(\boldsymbol{\eta})]$ established above will form the basis for obtaining the final covariances of the attitude vector expressed in terms of its right ascension λ and declination δ.

Linear Observation Model

The observation model connecting the angles η to the attitude unit vector Z is (cf., Fig. 1)

$$Z\cdot S=\cos\theta$$

$$Z\cdot E=\cos\beta$$

$$Z\cdot(S\times E)=\sin\theta\,\sin\beta\,\sin\alpha \tag{36}$$

Designating the right-hand sides by the vector $Y(\eta)$, Eqs. (36) can be expressed as a linear observation model

$$Y(\eta)=[H]Z \tag{37}$$

with

$$[H]=\begin{bmatrix} S_1 & S_2 & S_3 \\ E_1 & E_2 & E_3 \\ S_2E_3-S_3E_2 & S_3E_1-S_1E_3 & S_1E_2-S_2E_1 \end{bmatrix} \tag{38}$$

Here, S_j and E_j, $j=1,2,3$, denote the components of the satellite/sun and satellite/Earth unit-vectors in the inertial reference frame.

The covariance matrix $[\mathrm{cov}(Y)]$ can be calculated from $[\mathrm{cov}(\eta)]$:

$$[\mathrm{cov}(Y)]=[Q]\cdot[\mathrm{cov}(\eta)]\cdot[Q]^T \tag{39}$$

with

$$[Q]=\left[\frac{\partial Y}{\partial\eta}\right]=\begin{bmatrix} -\sin\theta & 0 & 0 \\ 0 & -\sin\beta & 0 \\ \cos\theta\,\sin\beta\,\sin\alpha & \sin\theta\,\cos\beta\,\sin\alpha & \sin\theta\,\sin\beta\,\cos\alpha \end{bmatrix} \tag{40}$$

It may be emphasized that the model in Eq. (37) is exact and avoids the cumbersome linearizations required in the case where the angles θ, β, and α themselves are taken as the observation inputs in the state estimation filter.

Attitude Vector Covariances

The effect of systematic biases on the attitude estimation result may be assessed by considering a single-frame attitude determination. This result would then be indicative of the systematic error remaining in the state estimate based on measurements in the immediate neighborhood of the selected time.

By performing the calculation for a number of points over the sensor coverage interval an assessment of the expected attitude determination error evolution over the coverage period can be performed.

The covariance matrix for the three inertial components of the attitude vector Z can be obtained by inverting the linear relationship in Eq. (37). Thereto, unitvectors T and N are introduced so that T lies in the plane formed by S and E, and N is normal to this plane as follows:

$$E=\cos\psi S+\sin\psi T,\quad S\times E=\sin\psi N \tag{41}$$

The matrix $[H]$ of Eq. (38) can now be decomposed as

$$[H]=\begin{bmatrix} 1 & 0 & 0 \\ \cos\psi & \sin\psi & 0 \\ 0 & 0 & \sin\psi \end{bmatrix}\begin{bmatrix} S_1 & S_2 & S_3 \\ T_1 & T_2 & T_3 \\ N_1 & N_2 & N_3 \end{bmatrix} \tag{42}$$

Inversion of this matrix can readily be performed because the second matrix in Eq. (42) is orthonormal,

$$[H]^{-1}=\frac{1}{\sin\psi}\begin{bmatrix} S_1 & T_1 & N_1 \\ S_2 & T_2 & N_2 \\ S_3 & T_3 & N_3 \end{bmatrix}\begin{bmatrix} \sin\psi & 0 & 0 \\ -\cos\psi & 1 & 0 \\ 0 & 0 & 1 \end{bmatrix} \tag{43}$$

It is noted that the components T_j and N_j, $j=1,2,3$, are known from the knowledge of S and E via Eqs. (41). The 3×3 covariance matrix of the three inertial attitude vector components now follows immediately:

$$[\mathrm{cov}(Z)]=[H]^{-1}\cdot[\mathrm{cov}(Y)]\cdot[H^{-1}]^T \tag{44}$$

This result illustrates the colinearity problem arising when $\psi\to0$ or π (when the vectors E and S become aligned). The matrix $[H]$ of Eq. (42) becomes singular in this case and the attitude becomes indeterminate. Since in a near-colinearity case the Earth and sun sensors provide good information only on the attitude component along the $S\sim\pm E$ reference direction, the projection of the attitude vector in the plane normal to this direction remains practically unobservable. For the covariance analysis it is important to recognize that the magnification of the systematic errors in sensor measurements into the final attitude result grows enormously for values of φ near 0 or π. It may be mentioned that the so-called dynamic attitude reconstitution method[4] has been developed with the purpose of resolving this difficulty by introducing a new reference direction along the vector $\dot{E}$.

Right Ascension and Declination Covariances

The final transformation to be implemented expresses the covariance matrix for the two angles λ and δ in terms of the covariances of the attitude vector inertial components. Using

$$\lambda=\arctan(Z_2,Z_1),\quad \delta=\arcsin(Z_3) \tag{45}$$

the linearized transformation

$$\begin{bmatrix} \Delta\lambda \\ \Delta\delta \end{bmatrix}=\begin{bmatrix} -Z_2/(Z_1^2+Z_2^2) & Z_1/(Z_1^2+Z_2^2) & 0 \\ 0 & 0 & 1/\sqrt{(1-Z_3^2)} \end{bmatrix}=[K]\Delta Z \tag{46}$$

can be established. The covariance matrix of λ and δ follows as:

$$[\mathrm{cov}(\lambda,\delta)]=[K]\cdot[\mathrm{cov}(Z)]\cdot[K]^T \tag{47}$$

This represents the final result in the chain of covariance transformations starting with the selected input biases and leading all the way up to the corresponding attitude vector right ascension and declination errors.

Discussion of Results

The covariance analysis presented herein is used routinely for attitude determination accuracy assessments for ESA's geostationary satellites in transfer orbit. For the purpose of illustration, a few typical results are shown in the accompanying figures which are based on the calculation of the covariances at 1-deg steps in true anomaly over the complete pencil-beam coverage interval. As input biases the values given in Eqs. (3) and (5) have been chosen in all cases. The extent of the coverage intervals of the individual pencil beam is indicated in the figures by the numbered bars. It is evident that the accuracy of the attitude determination improves considerably when both beams have coverage because of the optimal combination of the individual measurements.

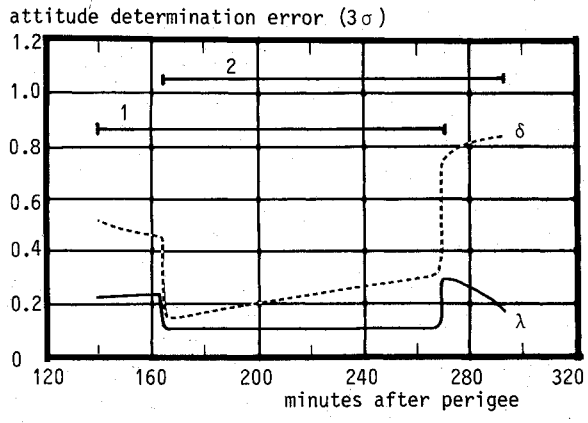

Fig. 8 Expected attitude determination error (3σ) for the same situation as in Fig. 7, but at sensor settings of 13.5 and 9.5 deg (refer to Fig. 6 for clarifications).

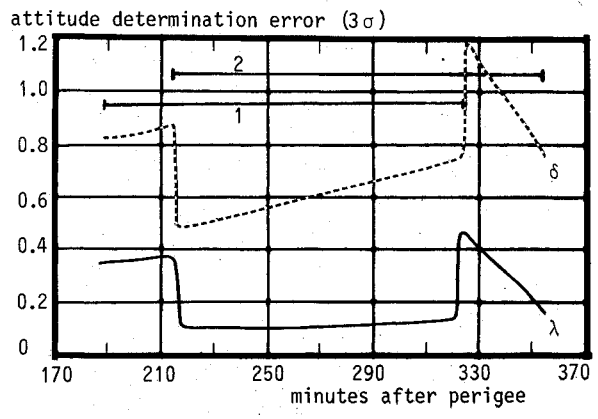

Fig. 9 Expected attitude determination error (3σ) for actual MARECS-A conditions, i.e., launch on December 20, 1981, and reference attitude λ = 2.5 deg, δ = −6.3 deg. Sensor settings are 11.5 and 7.5 deg (refer to Fig. 6 for clarifications).

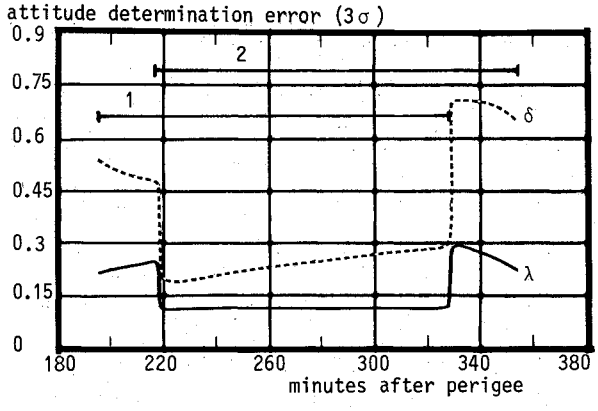

Fig. 10 Expected attitude determination error (3σ) for actual ECS-1 conditions, i.e., launch on June 16, 1983, and reference attitude λ = 336.6 deg, δ = −9.0 deg. Sensor settings are 6.5 and 2.5 deg (refer to Fig. 6 for clarifications).

Figure 6 shows the accuracy degradation due to a sun/Earth near-colinearity with a minimum ψ angle of about 4 deg at 254 min after perigee. A typical Ariane transfer orbit with parameters $a = 24{,}400$ km; $e = 0.73$; $i = 8.1$ deg; $\omega = 158.5$ deg; $\Omega = 210$ deg is considered. The pencil-beam settings are at -0.5 and -4.5 deg from the spacecraft equatorial plane. Acceptable attitude determination accuracies are assumed to be achievable when over an interval of 1 h the average 3σ declination error is below 0.6 deg and that of the right ascension is below 0.2 deg. In Fig. 6 this would be the case only for an interval extending far beyond apogee (occurring at 316 min). This is undesirable from an operational point of view. By selecting higher sensor settings it would be possible to shift the coverage interval closer to the perigee. In that case, however, the near colinearity would occur closer to the middle of the coverage interval and a serious degradation in attitude determination accuracy would result. In this case, acceptable accuracies may be achieved by shifting the longitude of the nodes (and thus launch time) such that the near colinearity occurs after apogee or still closer to perigee.

Since the sun/Earth angle represents one of the main factors governing the attitude determination accuracy, the location of the sensor coverage interval relative to the point of smallest sun/Earth angle is of extreme importance for the achievable accuracy in a particular launch configuration. For present ESA communication satellites it is possible to select a favorable sensor setting (out of a range of 19 deg) in order to avoid a sharp near-colinearity within the coverage interval during a given launch window. It is of interest to point out that, also in normal circumstances (i.e., when no colinearity problems are present), advantage could be taken of the available variable sensor mountings. This is illustrated in Figs. 7 and 8 for a launch on May 15 under identical transfer orbit conditions but with different pencil-beam settings. The sun/Earth angle decreases continually cover the coverage interval. A comparison of the two figures at 250 min clearly shows the upward trend in declination error for the decreasing sun/Earth angle. Although both settings would produce acceptable accuracies, there is a difference in the best 1-h averaged declination errors: 0.31 deg in Fig. 7 compared to 0.19 deg in Fig. 8. The corresponding expected fuel savings for acquisition maneuvers could amount to one month North-South stationkeeping which would increase the prospective mission lifetime by the same amount. From these considerations it is evident that the higher sensor setting is more favorable in this case.

There is an additional aspect that should be taken into account, namely, the evolution of the attitude determination error over the launch window. Table 1 provides a summary of the best 1-hr averaged declination errors for three different sensor settings (including the two cases illustrated in Figs. 7 and 8) over the launch window extending from 12 to 14 hr GMT. The expected error in right ascension is not relevant here as it lies between 0.13 and 0.14 deg in all cases considered. Since it is more likely that the launch would take place at the beginning rather than at the end of the launch window, the results of Table 1 should be weighted accordingly for selecting the best overall setting. In the present example the highest setting is the best also under these considerations.

Figure 9 shows the results of the covariance analysis for the actual transfer orbit conditions in the case of MARECS-A launch on December 20, 1981. The orbital elements were $a = 24{,}370$ km, $e = 0.73$, $i = 10.56$ deg, $\omega = 175$ deg, and $\Omega = 273.7$ deg. The fact that the expected attitude error as shown in Fig. 9 is relatively large is mainly due to the severe sensitivity of the attitude vector (in particular, its Z component) to errors in the sun/Earth azimuth angle: In terms of Wertz' (Sec. 10.5) terminology[1] the attitude vector lies close to the null point, i.e., near the direction of the $S \times E$ vector. This effect becomes progressively stronger over the coverage interval. The actual attitude determination error, which was reconstructed a posteriori from the orbits determined prior to and after apogee boost motor (ABM) firing, turned out to be on the order of 1 deg for MARECS-A.

Figure 10 illustrates the covariance results for the actual ECS-1 transfer orbit conditions ($a = 24{,}420$ km, $e = 0.73$, $i = 8.6$ deg, $\omega = 178$ deg, and $\Omega = 249.4$ deg) on June 16, 1983. In this case no particular sensitivity problems were observed, thus, the expected accuracy is relatively good. In fact, the ac-

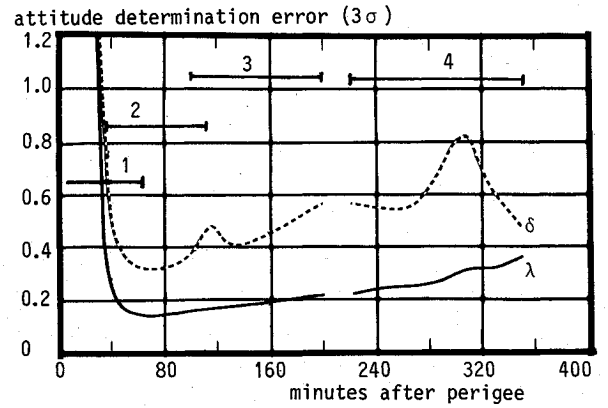

Fig. 11 Expected attitude determination error (3σ) for hypothetical Giotto launch configuration on July 5, 1985, and reference attitude $\lambda = -22.4$ deg, $\delta = -11.3$ deg. Sensor settings are ± 10 and ± 30 degs (refer to Fig. 6 for clarifications).

tually observed attitude error at ABM firing proved to be only 0.16 deg.

Finally, Fig. 11 shows the evolution of the expected attitude determination accuracy for ESA's Giotto spacecraft which has been launched by Ariane in a standard geostationary transfer orbit before being injected into its Halley's comet intercept trajectory by a perigee kick. This spacecraft is equipped with four pencil-beam sensors at fixed orientations ± 10 and ± 30 deg from the satellite's equator. The figure shown is valid for the launch on July 5, 1985, with the usual orbital elements and $\Omega = 284$ deg. The attitude is taken as $\lambda = -22.4$ deg and $\delta = -11.3$ deg. Figure 11 shows that an accuracy of 0.4 deg in declination and 0.2 deg in right ascension is achievable under the assumed conditions. In fact, Giotto was launched on July 2, 1985, with a near-perfect attitude determination result.

Concluding Remarks

A covariance analysis providing the expected attitude determination accuracies on the basis of realistic input biases in the fundamental sensor measurements has been presented. The results of this analysis allow one to select the most favorable attitude determination periods within a given coverage interval. In the case of satellites equipped with variable sensor mountings, as is the case with present-day communication satellites, the best possible sensor setting over a given launch window can be identified. The benefits of a more accurate attitude determination capability are apparent, as any fuel saved during orbit corrections needed because of attitude errors at apogee motor firing translates directly in a prolongation of the prospective mission lifetime. Finally, the results would provide a quantitative estimate on the achievable attitude determination accuracy on the basis of specified sensor measurement error tolerances.

Acknowledgment

The author wishes to express his gratitude to Dr. L. Fraiture for helpful discussions related to this study.

References

[1]Wertz, J.R., ed., *Spacecraft Attitude Determination and Control*, Reidel Publishing Co., Dordrecht, the Netherlands, 1978.

[2]Shuster, M.D., "Efficient Algorithms for Spin-Axis Attitude Estimation," *The Journal of the Astronautical Sciences*, Vol. 31, No. 2, April-June 1983, pp. 237-249.

[3]Van der Ha, J.C., "Attitude Determination Covariance Analysis for Geostationary Transfer Orbits," *OAD Working Paper No. 218*, European Space Operations Centre/ESA, March 1983.

[4]Bird, A.G., Fraiture, L., Van der Ha, J.C., and Kohler, P., "The Dynamic Attitude Reconstitution Method," *Proceedings of Spacecraft Flight Dynamics Symposium*, Darmstadt, FRG, May 1981; ESA SP-160, Aug. 1981, pp. 353-360.

AIAA Meetings of Interest to Journal Readers*

Date	Meeting (Issue of *AIAA Bulletin* in which program will appear)	Location	Call for Papers†
1986			
April 14-16	**Ballistic Missile Future Systems and Technology Workshop** (Feb.)	Norton AFB San Bernardino, CA	July 85
April 29-May 1	**AIAA Annual Meeting** (Feb.)	Hyatt Regency Crystal City Arlington, VA	
May 19-21	**AIAA/ASME/ASCE/AHS 27th Structures, Structural Dynamics and Materials Conf.** (March)	Marriott Hotel San Antonio, TX	May 85
June 18-20‡	**American Control Conference**	Seattle Sheraton Hotel Seattle, WA	
Aug. 18-20	**AIAA Guidance, Navigation and Control Confence** (June)	Williamsburg Hilton Williamsburg, VA	Nov 85
Aug. 18-20	**AIAA/ASS Astrodynamics Conference** (June)	Williamsburg Hilton Williamsburg, VA	Nov. 85
Aug. 18-21	**AIAA Atmospheric Flight Mechanics Conference** (June)	Williamsburg Hilton Williamsburg, VA	Nov. 85

*For a complete listing of AIAA meetings, see the current issue of the *AIAA Bulletin*.
†Issue of *AIAA Bulletin* in which Call for Papers appeared.
‡Co-sponsored by AIAA. For program information, write to: AIAA Meetings Department, 1633 Broadway, New York, N.Y. 10019.